A First Constraint on Basal Melt-water Production of the Greenland Ice Sheet

Nanna B. Karlsson[1,*], Anne M. Solgaard[1], Kenneth D. Mankoff[1], Jason E. Box[1], Michele Citterio[1], William T. Colgan[1], Signe H. Larsen[1], Kristian K. Kjeldsen[1], Niels J. Korsgaard[1], Douglas I. Benn[2], Ian Hewitt[3], and Robert S. Fausto[1]

[1]Geological Survey of Denmark and Greenland, Copenhagen, Denmark
[2]School of Geography & Sustainable Development, University of St. Andrews, St. Andrews, UK
[3]Oxford Centre for Industrial and Applied Mathematics, University of Oxford, Oxford, UK
[*]Corresponding author: nbk@geus.dk

The Greenland ice sheet is one of the largest sources of sea-level rise since the early 2000s. Basal melt has not been included explicitly in assessments of ice-sheet mass loss so far. Here, we present the first full-coverage estimate of the ice-sheet wide basal melt in Greenland and its recent change through time. We find that presently basal melting contributes at least 22.3 +5/-3 Gt per year to the total mass loss, and we estimate that basal melting has increased by at least 2.3 $\pm$0.8 Gt (or 12%) since 2000. The basal melt discharge from Sermeq Kujalleq (Jakobshavn Isbræ) has increased by 24 % in the same period. As the Arctic warms, basal melt will likely continue to increase thus aggravating current mass loss trends, enhancing solid ice discharge and modifying fjord circulation.

Introduction

Mass loss from the Greenland ice sheet is determined via one of three methods: through estimates of ice volume change from satellite altimetry[1, 2], by measuring changes in regional gravity due to mass loss[3] or by differencing between solid ice discharge and surface mass balance[4, 5] (the "input–output" method [6], the term solid ice discharge refers to the ice mass that exits through flux gates at the margin). Presently, the spread between different mass balance estimates is 24 Gt

per year corresponding to 10% of the imbalance[7]. Gravity methods implicitly include basal mass loss while altimetry methods attribute all mass loss to either ice discharge or surface mass loss. Both methods provide limited insights into the physical processes leading to the observed signal. In contrast, the input-output method relies on accurate process representation of the different mass-loss terms and thus provides a possibility for prediction of future changes. To date, the input-output method has overlooked basal mass balance entirely.

Constraining the basal melt term is important for three reasons. Firstly, uncertainty in the partition of ice-sheet mass loss between surface mass balance and ice discharge, including the failure to acknowledge the basal mass balance term, limits our understanding of changes in ice-sheet mass budget in response to recent climate change. This impedes our ability to capture complex interactions and feedbacks between ice sheets and the climate system. Secondly, recent studies have highlighted the importance of subglacial discharge for modifying the mass loss from marine-terminating glaciers. Subglacial discharge significantly increases the total submarine melt flux [8] and plays an equally important role as ocean temperatures for Greenland outlet glaciers' contribution to future sea-level rise[9]. Finally, discharge of subglacial water modifies circulation in the fjord systems and may impact the mixing of nutrients[10, 11].

Here, we provide the first estimate of ice-sheet-scale basal melt and its recent change through time. We consider three sources of basal heat (Fig. 1A-C). The first source, the geothermal flux, is assumed to be constant in time while the other terms, frictional heat and the heat from surface melt water, vary in response to changes in ice dynamics and surface melt. We quantify the basal melt using maps of geothermal flux, satellite-derived ice surface velocities, surface and bed topographies, and outputs from a regional climate model. We consider surface velocities from 2000/2001 as representative of ice-flow velocities prior to the onset of general speed-up of the ice sheet observed in the 2000s[4, 5]. Similarly, we consider average run-off volumes from 1960-1999 to be representative of surface melt water volumes before the present increase in surface melt. This allows us to construct a reference state against which we can compare basal melt rates derived from present day surface velocity (2018/2019) and run-off (average of 2010-2019). We use a decadal average for the run-off due to the high interannual variability of surface melt. We assume that all basal melt water is discharged to the ocean since the geometry and high surface slopes of the ice sheet preclude the existence of large subglacial lakes[12]. Although studies have found evidence of subglacial lakes[13, 14] and "units of disturbed radio-stratigraphy" [15, 16] both phenomena are of an extent that volumes are negligible in the context considered here. Our results demonstrate that basal melt is a non-negligible component of the mass loss from the Greenland ice sheet, and that the outflux of basal melt water is increasing and likely will continue to increase in the future.

Results

Geothermal flux contribution to basal melt

The heat from the geothermal flux is based on an average of three geothermal flux maps[17, 18, 19] and is masked with an independent estimate of where basal ice is likely at pressure melting point[20] (Fig. 1A, black and grey contours). Our estimate of total geothermal basal melt is 5.3 +4.0/-1.4 Gt per year. The uncertainty is due to the unknown basal temperature of the ice and our upper uncertainty bound represents the (unlikely) scenario that the entire ice sheet is at pressure melting point at the base. In comparison, the disagreements between the geothermal flux datasets can be large on local scales but translate into a small difference in basal melt. We find that the difference in ice-sheet-wide basal melt between the datasets are < 10 % and we therefore ignore uncertainties from the geothermal flux datasets. Studies suggest that the geothermal flux is generally underestimated in the northeastern (NE) sector due to the presence of a localised, "hot spot" under the North East Greenland ice stream[21, 22]. Therefore, our estimate comes with the caveat that the contribution from the NE sector is likely larger than the estimate presented here.
Spatially, the basal melt caused by geothermal flux is relatively evenly distributed (Fig. 1 D, Table 1). The highest melt rates are found in the central eastern (CE) sector where basal melt in a few places exceeds 0.01 m per year. In the CE, SW (southwestern) and SE (southeastern) sectors, melt rates are typically 0.006-0.007 m per year, while melt rates for the remaining sectors are 0.005 m per year or less. We assume that there is no contribution to the geothermal basal melt in the interior of the ice sheet, where basal ice is likely below the pressure melting point[20].

Frictional heat contribution to basal melt

The frictional heat is produced by ice sliding over the bed. This heat term is found by assuming that basal sliding is equal to the difference between observed winter surface velocities (Fig. 1B) and deformational (creep) velocities. The latter is calculated using a simplified stress-balance equation[23]. We estimate that the minimum total friction-induced basal melt is 13.0 +3.4/-3.5 Gt per year for present-day and 11.8$\pm$3.4 Gt per year for our reference period (Table 1) corresponding to a 10 % increase (Table 2). The parts of the ice sheet that experience basal melt rates above 0.01 m per year increased from 16 % (by area) to 18 % (blue contours, Fig. 1E). Furthermore, 5 % of grid points, all located along the margin, show a change in melt rates > 0.1 m during this time. Uncertainties for the frictional heat are dominated by the unknown temperatures of the deforming ice. Additional uncertainties stem from the velocity datasets, our use of a simplified stress-balance equation that provide a first-order approximation to the stress field[23], and the fact that our calculations are based on winter velocities leading to an underestimation of basal melt rates (summer velocities are typically higher). See methods for a detailed discussion of these uncertainties.
Melt from frictional heating is concentrated in areas with high ice-flow velocities i.e. at major

glacier outlets (cf. Fig. 1B). Most of the basal water is drained through large ice streams and eight of the major outlets have fluxes exceeding 10^6 t per year. In the slow-flowing interior, friction melt rates are typically at least an order of magnitude lower. In the northern (NO) sector, the outlet of Petermann Gletsjer is visible as an extended area where friction melt exceeds 0.01 m per year. Near the margin, melt rates approach 0.2 m per year. In the NE sector, most of the friction melt is generated by Nioghalvfjerdsfjorden glacier and Zachariae Isstrøm, and rates exceed 0.3 m per year close to the margin. High friction melt rates are also found in the CE and SE sectors where Kangerlussuaq Glacier and Helheim Glacier cause friction melt in excess of 0.4 m per year. In these two sectors, friction melt rates exceeding 0.01 m per year also extend inland. Basal friction as a source of melt is less significant in the slow-flowing sectors. In the predominantly land-terminating southwestern (SW) sector friction melt does not exceed 0.2 m per year. The central western (CW) sector has the largest areal extent of high friction melt rates and experiences melt rates above 0.4 m close to the margin. High friction melt in the CW sector is in part due to Sermeq Kujalleq (Jakobshavn Isbræ), one of Greenland's largest outlet glaciers. In contrast, the northwestern (NW) sector contain numerous smaller glaciers but combined they also create a large area where melt rates exceed 0.01 m per year.

Surface-melt water heat contribution to basal melt

Finally, we consider the heat generated by surface melt water as it infiltrates the subglacial system (Fig. 1C), and we convert the gravitational potential energy of melt water into either sensible heat, which increases water temperature, or latent heat, which melts open subglacial conduits as water flows through the ice sheet. This heat source has been calculated in previous studies[24] using surface water volumes from a regional climate model[25] but not translated directly into melt rates. We estimate that the average basal melt due to surface-melt water injection was on average 2.7$\pm$0.4 Gt per year in 1960-1999, while present-day values are 4.1$\pm$0.6 Gt per year (average from 2010-2019). Uncertainties stem from the 15 % uncertainty from the regional climate model. This change in basal melt corresponds to an increase of 50 % (Table 2.

The surface melt water contribution to basal melt is focussed in areas where surface melt occurs and runoff is generated, and where this runoff is subjected to large hydropotential gradients as it flows along the ice-sheet bed (Fig. 1 F). The basal melt rates are substantially higher than the geothermal basal melt rates along the high-gradient ice-sheet periphery but lower in the interior. The largest mass loss due to surface melt-water heat occurs in the SE and SW sectors (Table 1). The basal melt rates due to surface melt water exceed 0.05 m per year in a few places (< 1 %) along the margin but the bulk of the sectors experience melt rates below 0.0005 m per year. In contrast to the geothermal and frictional terms, the melt due to surface melt water is focused in the conduits and thus highly localised. The values reported above represent an average over 5 km grid cells masking the fact that melt rates vary orders of magnitude over sub-kilometre distances.

Total basal melt on regional and local scales

The present basal discharge is at least 22.3 +5.6/-4.0 Gt per year equivalent to 5.4 % of the annual solid ice discharge (average of 1986–2018 ice discharge[5]) or 16 % of surface mass loss (during 2012-2017 [7]). It also corresponds to approximately half of the annual discharge of Sermeq Kujalleq (average of 1986–2018 discharge[5]). At ice-sheet scale, basal melt is primarily caused by frictional heating (58 %), with surface-melt water heat and geothermal heat as secondary contributors (24 % and 18 %, respectively, Fig. 2B and Table 1). The individual contribution from each of the heat terms varies for the different ice-sheet sectors depending on local geothermal heat anomalies and surface melt water volumes. For example, in the slow-flowing SW sector the relative contributions from the three heat terms approach parity, while friction heat dominates in the CW and NW sectors (Table 1).

The basal-melt contribution to the total mass loss during our reference period is estimated at 19.9 +5.6/-4.0 Gt per year. Comparisons with present-day melt reveals an increase during the last two decades of 2.3$\pm$0.8 Gt or 12 % in basal melt discharge (Table 1). The contribution from friction melt has increased by 1.1 +0.08/-0.1 Gt while basal melt due to surface melt water has increased by 1.3 $\pm$0.7 Gt (Table 2). The latter represents an increase of 50% between our reference period and present day. The increase in friction melt appears to be constant during the last 15 years (Fig. 3). A linear regression through the velocity datasets from 2005/2006 through 2017/2018 indicates that basal friction discharge has increased by 0.09 +0.07/-0.06 Gt per year. The increase is due to speed up of several glacier outlets, where basal melt is spatially concentrated.

For individual sectors, all sectors with the exception of NO sector have experienced an increase in friction melt and all sectors have experienced an increase in melting caused by surface melt water (Fig. 4, Table 2). In the CE and SE sectors, the surface melt water contribution is now larger than the geothermal flux contribution (Fig. 4). The largest total change is seen in the CE and CW sectors, where basal melt has increased by 18 % due to an increase in both friction melt (9 % and 18%, respectively) and surface melt water contribution (64% and 55 %, respectively). The smallest change is found in the NO sector, where total basal melt increased by 6 % in spite of a 170 % increase in basal melt caused by surface melt water. We note that in order to represent basal mass loss on sector basis, the subglacial drainage basins are here assumed identical to the glaciological drainage basins.

On drainage-basin scales, a better stress-approximation is needed in order to obtain the basal melt from friction heat in glacier outlets smaller than several tens of kilometres. Therefore, we only present the basal melt discharge for three of the largest glaciers (by discharge and flux gate size): Sermeq Kujalleq, which discharges into Qeqertarsuup tunua (Disko Bay), Kangerlussuaq Glacier that discharges into Kangerlussuaq Fjord and Helheim Glacier that terminates in Sermilik Fjord. Here, we calculate the individual subglacial basins using the hydropotential[26]. We estimate that at present, the basal melt water flux from Sermeq Kujalleq is at least 2.3 +0.3/-0.6 Gt per year and

50 % of the basal melt water from the CW sector exits through Sermeq Kujalleq into Qeqertarsuup tunua. Compared to reference values of 1.9 +0.3/-0.6 Gt per year this corresponds to an increase of 24 %, implying that the influx of basal melt water into the fjord has increased significantly. At Kangerlussuaq Glacier the basal discharge at present is 1.0 $\pm$0.3 Gt per year, corresponding to 42% of the basal melt water in the CE sector. In our reference period, basal discharge is estimated at 0.8$\pm$0.3 Gt per year, an 18 % increase. Notably, we estimate that within our uncertainty range there has been no change in the basal discharge at Helheim Glacier, where present basal melt corresponds to 0.7 +0.3/-0.1 Gt per year (22 % of discharge in SE sector), despite observed speed up in recent years[5].

Discussion

We have shown that the volume of basal melt water from the Greenland ice sheet can be resolved and that it is a non-negligible part of the total mass budget. With a total mass balance of -251$\pm$63 Gt per year [7], basal discharge is presently equivalent to 9 % of this imbalance but is not included in input-output estimates of total mass loss. Basal melt is dynamic and will increase as the Greenland ice sheet responds to a warming climate. The frictional heat will likely increase as increasing ocean temperatures and surface melt lead to acceleration and increased areal extent of the fast-flowing regions[4]. Faster flow will increase basal melt production and lead to a larger mass loss. Since the response of large ice streams that control parts of the basal melt budget remains poorly understood, we cannot predict by how much the friction term will increase. Based on the recent past (Fig. 3), if glaciers continue to accelerate, basal melt water production may increase by $\sim$1 Gt every year in the foreseeable future. Heat generated by surface melt water will increase with increasing volumes of surface melt run-off. Under a business-as-usual future emission scenario this melt source will experience a dramatic 5-to-7-fold increase by 2100[24]. Thus, the overall mass loss associated with increasing surface melt will be further enhanced by the additional basal melt caused by the viscous heat dissipation from the surface melt water.

Basal melting may have a disproportionately large effect on ice-sheet and fjord processes. The basal discharge that stems from winter velocity frictional heat and geothermal flux is generated independently of air temperatures. Thus, the basal melt introduced and quantified here is the primary source of winter subglacial discharge, and this influx of winter basal water is poorly understood and sparsely measured[27]. Biological productivity is affected by subglacial discharge that modifies mixing in the fjords[11] but the impact of increasing winter freshwater on Arctic fjord environments is as-yet unknown. A modelling study of a glacier in West Greenland suggests that winter basal discharge may drive year-round submarine plumes leading to persistent ice-front melting, and that basal discharge may pull in warm water from the Atlantic further enhancing frontal melt rates[28]. Finally, recent and future increases in basal melting is likely to

have a non-linear effect on ice-sheet discharge. The projected contribution to sea-level rise from the Greenland ice sheet is significantly larger when subglacial discharge is increased, and this effect is comparable to the increase caused by rising ocean temperatures [9]. Thus, increasing basal melt will further aggravate mass loss from marine-terminating glaciers.

Methods

Surface and bed topographies

Our estimates are based on two different bed topographies and three different surface elevation datasets. We use the kriging-based bed topography published in 2013[29] and the bed topography from BedMachine v3 (BedMachine v2 for the surface water heat, the changes in subglacial routing from BedMachine v2 to v3 are negligible, especially given that results presented here are summed across large regions) calculated using a mass-conservation method[30]. Both datasets include a surface topography derived from GIMP (Greenland Ice sheet Mapping Project[31]) that spans a time period between 20 February 2003 to 11 October 2009. In addition, we use the surface topography from the Climate Change Initiative (CCI, http://cci.esa.int/) derived from the ArcticDEM (Arctic Digital Elevation Model[32]) based mainly on the WorldView 1-3 satellites. This gives a long temporal baseline from 2007 until present day. We combine the CCI surface elevation with the BedMachine v3 bed topography data. In all cases we apply an ice cover mask[33] in order to remove local ice caps and glaciers. The results presented as present-day are based on CCI surface elevation and BedMachine v3 bed topography.

Ice velocity data

We make use of two sources for ice velocity: The MEaSUREs (Making Earth System Data Records for Use in Research Environments) Greenland Ice Velocity data based on data from RADARSAT-1, ALOS, TerraSAR-X/TanDEM-X and Sentinel-1A and -1B[34, 35], and the PROMICE (Programme for Monitoring of the Greenland ice sheet) velocity product based on Sentinel-1A and -1B[36].
The MEaSUREs velocity maps cover the periods from winter 2000/2001 to winter 2017/2018 although the coverage is not continuous: Velocity maps are not available through 2001/2002 to 2004/2005. Only the latest velocity maps are complete and therefore we apply the same methodology as described in [5] and linearly interpolate missing values in time. We do not interpolate spatially since spatial changes are most likely larger than temporal changes for any given point. Data at the beginning or end of the time series are back- or forward-filled with the temporally nearest value for that grid cell.
The PROMICE dataset spans winter 2016/17 to winter 2018/19 and is based on intensity offset tracking. Here, the data coverage is near complete and no interpolation is necessary. We note that

the PROMICE maps overestimate the velocities in the interior of the ice sheet where MEaSUREs relies on the more accurate InSAR. The results presented as present-day are based on PROMICE winter velocities from 2018/2019.

Geothermal heat

We use the average geothermal flux from three published studies[17, 18, 19]. Note that one of the datasets (Fox Maule[17]) does not cover the southern tip of Greenland so here only the other two datasets are used. We calculate the resulting melt rates from the geothermal heat assuming that the ice is at pressure melting point. The result is then masked with a map of estimated basal conditions based on a combination of radar observations and model studies[20], where bed conditions were classified as either "frozen", "uncertain" or "thawed". Here, we assume that grid cells assigned as "frozen" do not contribute with any basal melt, grid cells assigned as "thawed" contribute fully to the basal melt. All "uncertain" grid cells contribute with 50 % of their potential basal melt. We can directly calculate the basal melt rate[23] as

$$\dot{b}_m = \frac{E_b}{\rho_i L} \tag{1}$$

where E_b is energy at the bed in this case, the geothermal flux, ρ_i is the density of ice, and L is the latent heat of fusion.

Overall, the largest uncertainty is the unknown basal temperature of the ice. If we assume that the bed of the entire ice sheet is at pressure melting point, the total geothermal melt component increases by more than 70 % (71 % - 78 %, depending on geothermal flux map). Conversely, if we assume that all areas are frozen where observations are ambiguous (Fig. 1B, grey contour), the total geothermal melt component decreases by approximately 26 % (26 % - 27 %).

Frictional heat

We estimate the frictional heating contribution using ice-sheet-wide surface-velocity maps. We use a simplified stress-balance equation coupled with the velocity observations to calculate the basal sliding velocity. On spatial scales over several ice thicknesses, ice flow can be assumed to consist of two components: deformational velocity u_d (at times also referred to as creep velocity) and basal sliding u_b [23]. Thus the total velocity is

$$u = u_d + u_b \tag{2}$$

and here we assume that u is equivalent to the observed surface velocity u_o. Our method thus retrieves the basal velocity from the observed surface velocity and the deformational velocity.

Theoretically, the surface velocity due to deformation is [23]

$$u_{s,def} = \frac{2A(T)}{n+1}\tau_b^n H \quad , \tag{3}$$

where $A(T)$ is the flow law parameter, H is ice thickness, n the flow law exponent, and $\tau_b = \tau_d = \rho g H \nabla s$, where ρ_i is ice density, g is gravity and ∇s is the surface gradient. We perform this calculation on a 10 km grid where ice surfaces have been smoothed by a 20 km running mean (the recommended smoothing in order to derive driving stresses is 8-10 ice thicknesses[37]) The flow law parameter $A(T)$ depends on temperature. Since most of the deformation takes place at the lower 20 % of the ice column, the appropriate value for A in our case is probably closer to the temperature at the bed than the average temperature of the ice column. We use internal ice temperatures derived from radar-attenuation values[38] to calculate the deformational velocities, and add a constant offset of 20°C (see supplementary material) to capture temperatures in the lower 20 % of the ice column where ice is warmer than the overlying ice[23]. From the theoretical deformational velocities we thus get our basal sliding velocity

$$u_b = u_o - u_{s,def} \tag{4}$$

and from this we can directly calculate the frictional heat and thereby the melt rate, assuming that the temperature of the ice is at pressure melting point:

$$\dot{b}_m = \frac{u_b\,\tau_b}{\rho_i L} \tag{5}$$

where L is latent heat of fusion of ice at 0°C.

In order to investigate the uncertainties in this approach, we vary our constant temperature offset by ± 5°C. This leads to a change in basal melt from frictional heat by $\mp$27 % (for 2018/2019) or $\mp$29 % (for 2000/2001). All other uncertainties are likely of secondary importance compared to this uncertainty range. In our analysis, the use of a simplified stress-balance equation provides a first-order approximation to the stress field[23]. This limits our horizontal resolution and may not resolve all the narrow (below 20 km wide) and fast flowing outlet glaciers. In addition, our calculations are based exclusively on winter velocities leading to an underestimation of basal melt rates since summer velocities are typically higher. Finally, recent observations of a borehole in western Greenland found that ice deformation was dominated by sliding in spite of slow ice flow[39]. Our simple analysis infers negligible basal sliding in slow-flowing areas. Consequently, these limitations imply that we are likely underestimating the frictional heat component of the total basal melt. It should be noted that gaps in the 2000/2001 velocity field is back-filled with data points from later observations where velocities are likely higher, thus the underestimation is partly countered by overestimating 2000/2001 velocities. The temporal change in basal melt is,

however, underestimated due to the back-filling.

The uncertainty in the change in basal melt is significantly smaller than the uncertainties associated with each year. Below, we outline how these uncertainties were found. We assume that the internal ice temperature is constant in time and thus the uncertainty from the unknown internal temperature is negligible when considering the change in basal melt. Instead, uncertainties for the change in friction melt are firstly, based on the difference in slope for the three temperature offsets (black lines in Fig. 3) and secondly on the uncertainty from the MEaSUREs velocity datasets. Note, that we only use datasets from years 2005/2006, 2007/2008, 2008/2009, 2009/2010, 2012/2013, 2014/2015, 2015/2016, and 2016/2017 to calculate the regression line shown in Fig. 3 because these datasets have less than 25% of back-filled grid points. The difference in slope for the three temperature offsets can be found straightforwardly by subtracting the slopes of the regression line. To translate the velocity uncertainty into friction-melt uncertainty, we perturb all points in the velocity datasets by a randomly selected number between -1 and 1 multiplied with the standard deviation for the point. We use the standard deviation that is given in the datasets by the data supplier. In this way, we generate 1000 perturbed velocity maps for each MEaSUREs dataset from the years 2005/2006, 2007/2008, 2008/2009, 2009/2010, 2012/2013, 2014/2015, 2015/2016 and 2016/2017. We then calculate the friction melt for each perturbed velocity map and find that this leads to a distribution of friction melt values where 95 % of values deviate less than ± 1 % from the mean value, and we therefore assign an uncertainty of ± 1 % caused by uncertainties in the velocity datasets. The total uncertainty is then found with simple error propagation (square root of the sum of squares for the two terms).

Subglacial water routing and viscous heat dissipation

We estimate the surface melt water contribution using previously published heat estimates[24] which are derived from MAR (Modèle Atmosphérique Régionale) v3.5.2 runoff[25], and hydrologic routing estimated from the BedMachine v2 digital elevation models[30].

We assume that the subglacial water follows the steepest gradient of the hydropotential[26] Φ

$$\Phi = \rho_w g z_b + \rho_i g (z_s - z_b) \ , \tag{6}$$

where ρ_w is the density of water, and z_b and z_s are the elevations of bed and surface topography, respectively.

As the basal melt water travels through the subglacial system it follows the hydropotential gradient, and energy is released. This energy Q is tracked and depends on the volume of water V, the change in hydropotential, and the change in phase transition temperature (last term)

$$Q = V \Big(\nabla \Phi - C_T c_p \rho_i \rho_w g \nabla (z_s - z_b) \Big) \quad , \tag{7}$$

where C_T is the Clausius–Clapeyron slope ($8.6{*}10^{-8}$ K Pa^{-1}), c_p the specific heat of water 4184 J K^{-1} kg^{-1}.

We assume that all potential energy is converted to heat[24], that surface water immediately penetrates to the bed and that the englacial water is at the pressure melting point, meaning that the viscous heat dissipation contribution to basal melt is effectively equivalent to the ice volume melted to form the en- and subglacial conduits[40]. The viscous heat dissipation is the sole reason why the surface melt water increases the basal melt rates. We include viscous heat dissipation in all three heat terms but for the frictional and geothermal heat terms, the viscous heat dissipation is negligible, and locally leads to less than 1 % increase in basal melt rates.

References

[1] Sørensen, L. S. *et al.* Mass balance of the greenland ice sheet (2003–2008) from icesat data – the impact of interpolation, sampling and firn density. *The Cryosphere* **5**, 173–186 (2011). URL https://www.the-cryosphere.net/5/173/2011/.

[2] McMillan, M. *et al.* A high-resolution record of greenland mass balance. *Geophysical Research Letters* **43**, 7002–7010 (2016).

[3] Velicogna, I., Sutterley, T. C. & van den Broeke, M. R. Regional acceleration in ice mass loss from greenland and antarctica using grace time-variable gravity data. *Geophysical Research Letters* **41**, 8130–8137 (2014).

[4] Mouginot, J. *et al.* Forty-six years of Greenland Ice Sheet mass balance from 1972 to 2018. *Proceedings of the National Academy of Sciences* (2019).

[5] Mankoff, K. D. *et al.* Greenland ice sheet solid ice discharge from 1986 through 2017. *Earth System Science Data* **11**, 769–786 (2019).

[6] Khan, S. A. *et al.* Greenland ice sheet mass balance: a review. *Reports on Progress in Physics* **78**, 046801 (2015).

[7] Shepherd, A. *et al.* Mass balance of the greenland ice sheet from 1992 to 2018. *Nature* (2019).

[8] Jackson, R. H. *et al.* Meltwater intrusions reveal mechanisms for rapid submarine melt at a tidewater glacier. *Geophysical Research Letters* **47**, e2019GL085335 (2020). URL https://agupubs.onlinelibrary.wiley.com/doi/abs/10.1029/2019GL085335. E2019GL085335 10.1029/2019GL085335, https://agupubs.onlinelibrary.wiley.com/doi/pdf/10.10

[9] Beckmann, J. *et al.* Modeling the response of greenland outlet glaciers to global warming using a coupled flow line–plume model. *The Cryosphere* **13**, 2281–2301 (2019). URL https://www.the-cryosphere.net/13/2281/2019/.

[10] Meire, L. *et al.* Marine-terminating glaciers sustain high productivity in greenland fjords. *Global Change Biology* **23**, 5344–5357 (2017). URL https://onlinelibrary.wiley.com/doi/abs/10.1111/gcb.13801.

[11] Hopwood, M. J. *et al.* Review article: How does glacier discharge affect marine biogeochemistry and primary production in the arctic? *The Cryosphere Discussions* **2019**, 1–51 (2019). URL https://www.the-cryosphere-discuss.net/tc-2019-136/.

[12] Pattyn, F. Investigating the stability of subglacial lakes with a full Stokes ice-sheet model. *Journal of Glaciology* **54** (2008).

[13] Palmer, S. J. *et al.* Greenland subglacial lakes detected by radar. *Geophysical Research Letters* **40** (2013).

[14] Bowling, J. S., Livingstone, S. J., Sole, A. J. & Chu, W. Distribution and dynamics of greenland subglacial lakes. *Nature Communications* **10** (2019).

[15] Bell, R. E. *et al.* Deformation, warming and softening of Greenland's ice by refreezing meltwater. *Nature Geoscience* (2014).

[16] Panton, C. & Karlsson, N. B. Automated mapping of near bed radio-echo layer disruptions in the Greenland Ice Sheet. *Earth and Planetary Science Letters* **432**, 323–331 (2015).

[17] Fox Maule, C., Purucker, M. E. & Olsen, N. Inferring magnetic crustal thickness and geothermal heat flux from crustal magnetic field models (2009).

[18] Shapiro, N. M. & Ritzwoller, M. H. Inferring surface heat flux distributions guided by a global seismic model: particular application to antarctica. *Earth and Planetary Science Letters* **223**, 213 – 224 (2004).

[19] Martos, Y. M. *et al.* Geothermal heat flux reveals the iceland hotspot track underneath greenland. *Geophysical Research Letters* **45**, 8214–8222 (2018). URL https://agupubs.onlinelibrary.wiley.com/doi/abs/10.1029/2018GL078289. https://agupubs.onlinelibrary.wiley.com/doi/pdf/10.1029/2018GL078289.

[20] MacGregor, J. A. *et al.* A synthesis of the basal thermal state of the Greenland Ice Sheet. *Journal of Geophysical Research: Earth Surface* **121**, 1328–1350 (2016).

[21] Fahnestock, M., Abdalati, W., Joughin, I., Brozena, J. & Gogineni, P. High Geothermal Heat Flow, Basal Melt, and the Origin of Rapid Ice Flow in Central Greenland. *Science* **294**, 2338–2342 (2001).

[22] Smith-Johnsen, S., Schlegel, N.-J., de Fleurian, B. & Nisancioglu, K. H. Sensitivity of the north-east greenland ice stream to geothermal heat. *Journal of Geophysical Research: Earth Surface* **125**, e2019JF005252 (2020).

[23] Cuffey, K. M. & Paterson, W. S. B. *The Physics of Glaciers* (Butterworth-Heinemann, 2010).

[24] Mankoff, K. D. & Tulaczyk, S. M. The past, present, and future viscous heat dissipation available for greenland subglacial conduit formation. *The Cryosphere* **11**, 303–317 (2017). URL https://www.the-cryosphere.net/11/303/2017/.

[25] Fettweis, X. *et al.* Estimating the greenland ice sheet surface mass balance contribution to future sea level rise using the regional atmospheric climate model mar. *The Cryosphere* **7**, 469–489 (2013). URL https://www.the-cryosphere.net/7/469/2013/.

[26] Shreve, R. L. Movement of water in glaciers. *Journal of Glaciology* **11**, 205–214 (1972).

[27] Pitcher, L. H. *et al.* Direct observation of winter meltwater drainage from the greenland ice sheet. *Geophysical Research Letters* **47**, e2019GL086521 (2020). URL https://agupubs.onlinelibrary.wiley.com/doi/abs/10.1029/2019GL086521. https://agupubs.onlinelibrary.wiley.com/doi/pdf/10.1029/2019GL086521.

[28] Cook, S. J., Christoffersen, P., Todd, J., Slater, D. & Chauché, N. Coupled modelling of subglacial hydrology and calving-front melting at store glacier, west greenland. *The Cryosphere* **14**, 905–924 (2020). URL https://www.the-cryosphere.net/14/905/2020/.

[29] Bamber, J. L. *et al.* A new bed elevation dataset for greenland. *The Cryosphere* **7**, 499–510 (2013).

[30] Morlighem, M. *et al.* BedMachine v3: Complete Bed Topography and Ocean Bathymetry Mapping of Greenland From Multibeam Echo Sounding Combined With Mass Conservation. *Geophysical Research Letters* **44**, 11,051–11,061 (2017).

[31] Howat, I. M., Negrete, A. & Smith, B. E. The greenland ice mapping project (gimp) land classification and surface elevation data sets. *The Cryosphere* **8**, 1509–1518 (2014). URL https://www.the-cryosphere.net/8/1509/2014/.

[32] Porter, C. *et al.* Arcticdem (2018). URL https://doi.org/10.7910/DVN/OHHUKH.

[33] Citterio, M. & Ahlstrøm, A. P. Brief communication "the aerophotogrammetric map of Greenland ice masses". *The Cryosphere* **7**, 445–449 (2013). URL https://www.the-cryosphere.net/7/445/2013/.

[34] Howat, I. MEaSUREs Greenland Ice Velocity: Selected Glacier Site Velocity Maps from Optical Images, Version 2. 0478, updated 2019. (2019). URL https://nsidc.org/data/NSIDC-0646/versions/2.

[35] Joughin, I., Smith, B. E., Howat, I. M., Scambos, T. & Moon, T. Greenland flow variability from ice-sheet-wide velocity mapping. *Journal of Glaciology* **56**, 415–430 (2010).

[36] Solgaard, A. M. & Kusk, A. Programme for monitoring of the greenland ice sheet (promice): Greenland ice velocity. (2019). URL http://promice.org/PromiceDataPortal/api/download/92ce7cf4-59b8-4a3f-8f75-93d166f5a7ca/

[37] McCormack, F. S., Roberts, J. L., Jong, L. M., Young, D. A. & Beem, L. H. A note on digital elevation model smoothing and driving stresses. *Polar Research* **38** (2019). URL https://polarresearch.net/index.php/polar/article/view/3498.

[38] MacGregor, J. A. *et al.* Radar attenuation and temperature within the greenland ice sheet. *Journal of Geophysical Research: Earth Surface* **120**, 983–1008 (2015). URL https://agupubs.onlinelibrary.wiley.com/doi/abs/10.1002/2014JF003418. https://agupubs.onlinelibrary.wiley.com/doi/pdf/10.1002/2014JF003418.

[39] Maier, N., Humphrey, N., Harper, J. & Meierbachtol, T. Sliding dominates slow-flowing margin regions, greenland ice sheet. *Science Advances* **5** (2019). URL https://advances.sciencemag.org/content/5/7/eaaw5406.

[40] Isenko, E., Naruse, R. & Mavlyudov, B. Water temperature in englacial and supraglacial channels: Change along the flow and contribution to ice melting on the channel wall. *Cold Regions Science and Technology* **42**, 53 – 62 (2005). URL http://www.sciencedirect.com/science/article/pii/S0165232X04001594.

[41] Mouginot, J. & Rignot, E. Glacier catchments/basins for the Greenland Ice Sheet (2019).

Acknowledgements

PROMICE is funded by the Geological Survey of Denmark and Greenland (GEUS) and the Danish Ministry of Climate, Energy and Utilities under the Danish Cooperation for Environment in the Arctic (DANCEA), and is conducted in collaboration with DTU Space (Technical University of Denmark) and Asiaq, Greenland. The authors gratefully acknowledge insights from S. Rysgaard (Aarhus University, Denmark) and M. Oksman (GEUS) on marine nutrients and primary production.

Author contributions statement

N.B.K. conceived the study in collaboration with A.M.S, D.I.B. and I.H. N.B.K. designed and ran the models. A.M.S. constructed the velocity data sets, K.D.M. calculated the surface melt water contribution. J.E.B. contributed to discussions of total mass balance. M.C. adapted an ice mask for the purposes of this study. S.H.L. assisted with error checking the code. W.T.C., R.S.F. and K.K.K. compiled mass budget information for comparison. N.J.K. assisted with figures. N.B.K. wrote the manuscript with input from all authors.

	Sector	Geothermal (Gt per year)	Friction (Gt per year)	Surface water (Gt per year)	Total melt (Gt per year)
Reference	Central east (CE)	0.5 +0.8/-0.3	1.1 +0.3/-0.5	0.4±0.1	2.0 +0.9/-0.5
	Central west (CW)	0.7 +0.5/-0.1	3.0 +0.6/-1.2	0.3±0.1	4.1 +0.8/-1.2
	Northeast (NE)	1.3 +0.7/-0.4	1.6 +0.2/-0.2	0.1±0.0	3.0 +0.7/-0.4
	North (NO)	0.4 +0.7/-0.2	0.7 +0.3/-0.1	0.1±0.0	1.3 +0.7/-0.3
	Northwest (NW)	0.6 +0.7/-0.2	2.6 +0.8/-0.8	0.3±0.0	3.4 +1.1/-0.8
	Southeast (SE)	0.7 +0.3/-0.2	1.7 +0.8/-0.3	0.7±0.1	3.1 +0.9/-0.4
	Southwest (SW)	1.2 +0.2/-0.1	1.1 +0.5/-0.3	0.8±0.1	3.1 +0.5/-0.3
	Total	**5.3 +4.0/-1.4**	**11.8 +3.4/-3.4**	**2.7±0.4**	**19.9 +5.6/-4.0**
Present	Central east (CE)	0.5 +0.8/-0.3	1.2 +0.3/-0.5	0.7±0.1	2.4 +0.9/-0.6
	Central west (CW)	0.7 +0.5/-0.1	3.6 +0.6/-1.2	0.5±0.1	4.8 +0.8/-1.2
	Northeast (NE)	1.3 +0.7/-0.4	1.8 +0.2/-0.2	0.2±0.0	3.2 +0.8/-0.4
	North (NO)	0.4 +0.7/-0.2	0.7 +0.3/-0.1	0.2±0.0	1.3 +0.7/-0.3
	Northwest (NW)	0.6 +0.7/-0.2	2.9 +0.8/-0.8	0.5±0.1	4.0 +1.0/-0.8
	Southeast (SE)	0.7 +0.3/-0.2	1.7 +0.8/-0.3	0.9±0.1	3.3 +0.9/-0.4
	Southwest (SW)	1.2 +0.2/-0.1	1.1 +0.5/-0.3	1.0±0.2	3.3 +0.5/-0.3
	Total	**5.3 +4.0/-1.4**	**13.0 +3.4/-3.5**	**4.1±0.6**	**22.3 +5.6/-4.0**

Table 1: Basal discharge from reference period and present-day in Gt per year. Our reference period covers winter 2000/2001 for the friction heat term and 1960-1999 for the surface meltwater heat term. Present-day is winter 2018/2019 for the friction heat term and 2010-2019 for the surface meltwater heat term. The table shows the melt from each sector and each heat terms. Note that melt due geothermal flux does not change.

		Change (Gt)	Change (%)
Source	Frictional	1.1 +0.08/-0.1	**10 +0.5/-0.8 %**
	Surface melt	1.3±0.7	**50±27 %**
	Total	2.3±0.7	**17±5 %**
Sector	Central east (CE)	0.4 ±0.1	18±6 %
	Central west (CW)	0.7 +0.09/-0.1	18 +2/-3 %
	Northeast (NE)	0.3 +0.03/-0.04	9±1 %
	North (NO)	0.07 ±0.04	6±3 %
	Northwest (NW)	0.6 ±0.09	16 +3/-2 %
	Southeast (SE)	0.2 ±0.2	8±6 %
	Southwest (SW)	0.3 ±0.2	8±6 %

Table 2: Change in friction melt and melt from surface melt water. Geothermal flux is not included because it is assumed to be constant in time. Lower part of table shows the change in basal melt by sector.

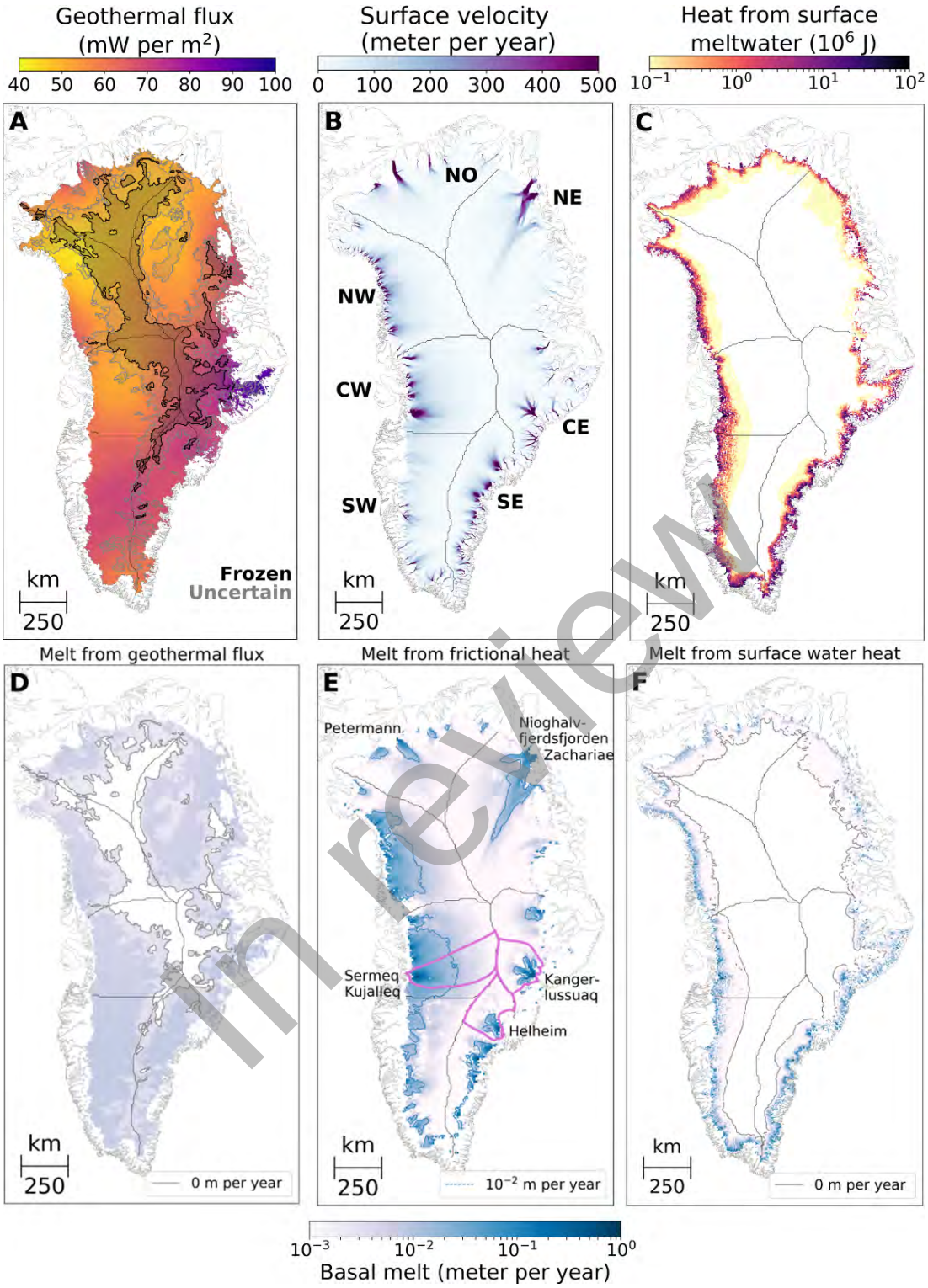

Figure 1: (A) Mean geothermal flux from [17, 18, 19]. (B) Surface velocities from winter 2018/2019 derived from Sentinel-1 data[36] The shaded areas outline where bed conditions are frozen (black) or uncertain (gray) based on radar observations[20] (C) Heat generated by surface melt-water infiltration. (D) Basal melting from geothermal heating. (E) Basal melting from frictional heating. Purple outlines show the glacial catchments of Sermeq Kujalleq, Kangerlussuaq and Helheim Glacier[41]. (F) Basal melting from surface water heating. (D), (E), and (F) have the same logarithmic scalebar.

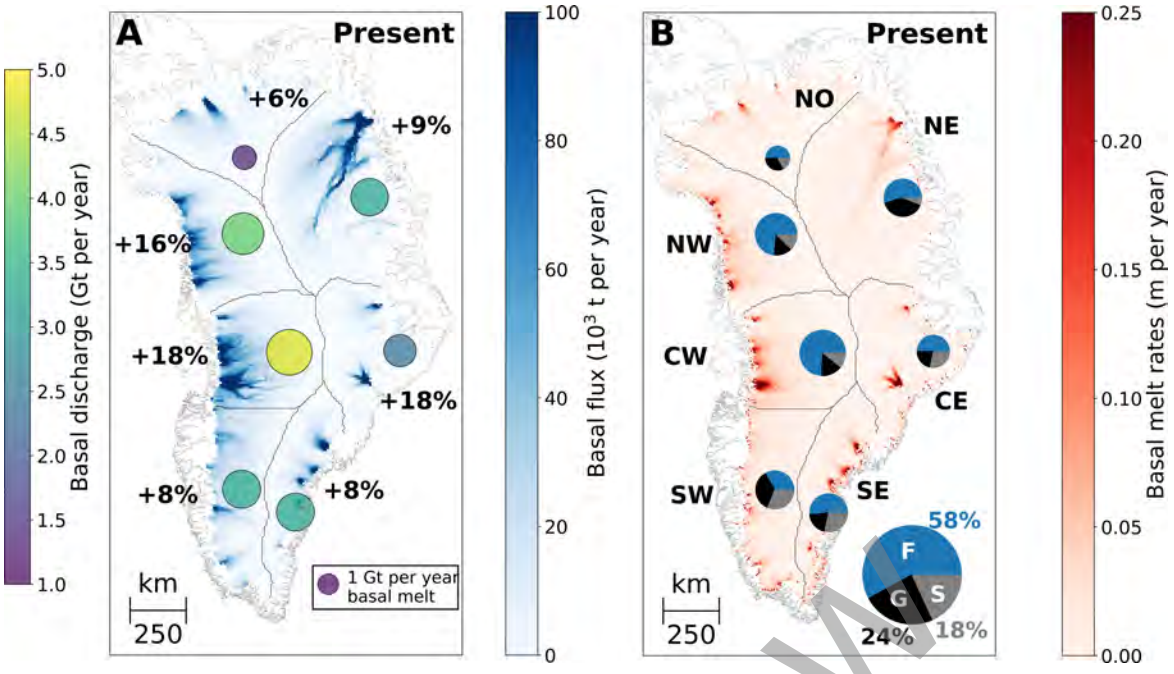

Figure 2: (A) Present day flux of basal melt water. Size and colour of circles indicate the total basal discharge from each sector. Numbers indicate percentage change compared to our reference period. (B) Basal melt rates for present day. Pie charts show the contribution from the different heat terms: friction heat (F, blue), geothermal flux (G, black) and viscous heat dissipation from surface melt water (S, grey). Size of circles indicate the total basal discharge from each sector.

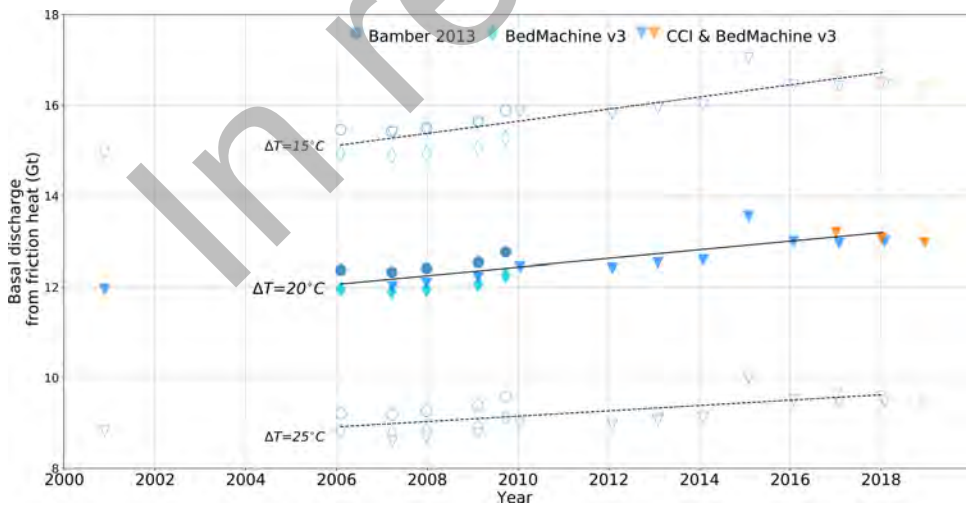

Figure 3: Basal melt discharge due to friction heat from winter 2000/2001 through to winter 2018/2019. Blue and turquoise colours indicate results based on the gap-filled MEaSUREs dataset (see methods). Orange colours indicate that results are from the PROMICE Sentinel-1 derived velocities. Black line is best linear fit through the MEaSUREs datasets (from the years 2005/2006, 2007/2008, 2008/2009, 2009/2010, 2012/2013, 2014/2015, 2015/2016 and 2016/2017), dashed black lines represent best linear fit if internal ice deformation temperatures are offset by ± 5°C. The shape of the points indicate origin of surface and bed topographies.

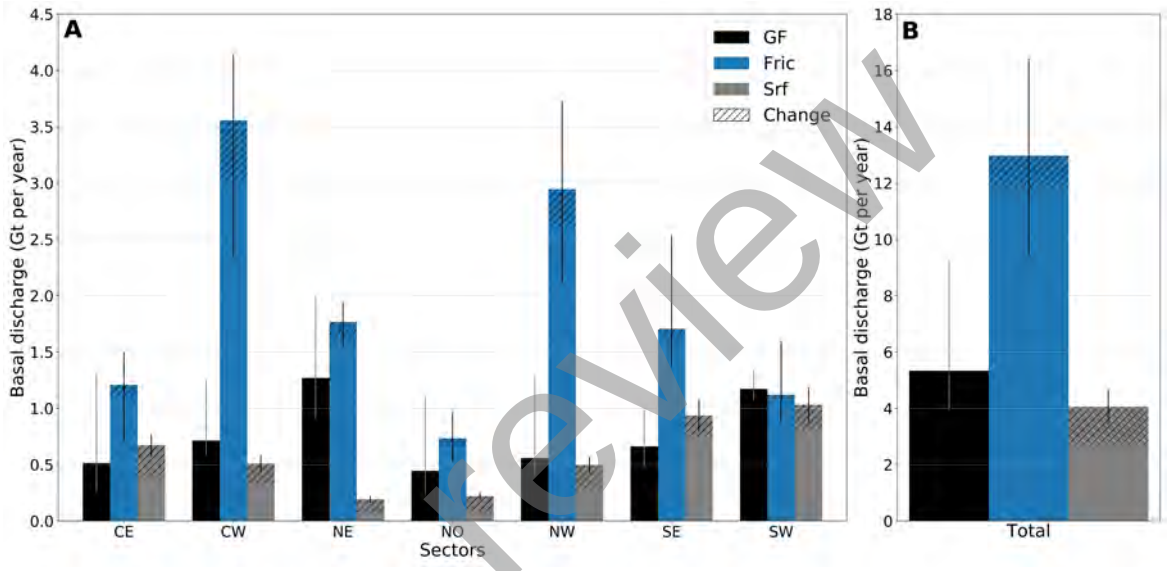

Figure 4: Figure illustrates the present-day contribution including uncertainties for each of the heat terms, while hatched area illustrate the increase from the reference period to the present-day. Colours indicate heat terms: Friction heat (blue), geothermal flux (black) and viscous heat dissipation from surface melt water (grey). (A) shows each sector and (B) the total basal melt discharge.